International Journal of Electrical and
Electronics Engineering Research (IJEEER)
ISSN(P): 2250-155X; ISSN(E): 2278-943X
Vol. 4, Issue 2, Apr 2014, 193-204

SENSORLESS POSITION CONTROL OF ZERO-SEQUENCE CARRIER INJECTION BASED PM SYNCHRONOUS MOTOR

P. RAM KISHORE KUMAR REDDY

Associate Professor, Department of EEE, MGIT, Hyderabad, Andhra Pradesh, India

ABSTRACT

A position sensorless control method for PM synchronous motors is proposed in this paper. It relies on the magnetic saliencies to estimate the position of the rotor. In usual sensorless methods, a signal is injected in the $\alpha\beta$ or dq components. In the proposed method, the signal is injected in the zero-sequence component. The high-frequency inherent zero-sequence component produced by a space-vector pulse width modulator (PWM) is used. In this way, no modification is required in the PWM, even at zero voltage, and the injected signal does not interact with the current controller. The response to the injected signal is obtained by a simple current derivative sensor. With this method, the position can be evaluated with high dynamics and with a high Signal-to-noise ratio. To further improve the performance of torque control switching table is entered by the imaginary voltage vector, which is generated from the DTC method for voltage source inverter, and the position of input voltage vector which can be measured. It can be observed that torque ripple has been reduced with the proposed DTC. Simulation results for three phase stator currents, d-q axes flux, estimated speed and torque are obtained and direct torque control with compensation and without compensation method is implemented.

KEYWORDS: DTC, PWM, PMSM

INTRODUCTION

A synchronous machine is an ac rotating machine whose speed under steady state condition is proportional to the frequency of the current in its armature. The magnetic field created by the armature currents rotates at the same speed as that created by the field current on the rotor, which rotates at the synchronous speed, and a steady torque results. Synchronous machines are commonly used as generators especially for large power systems, such as turbine generators and hydroelectric generators in the grid power supply. Because the rotor speed is proportional to the frequency of excitation, synchronous motors can be used in situations where constant speed drive is required.

The position of the rotor in electric machines by measuring only voltage and currents, evolved significantly in recent years [1]. Position of the rotor can be determined by the back electromotive force (EMF) or by the position dependence of the inductances. Position estimation based on the EMF cannot determine the position in standstill and they have low accuracy at low speed.

By using the position dependence of the inductances, the position can be determined also in standstill. The position dependence of the inductance, hereafter called magnetic saliency, is produced by saliencies in the rotor, magnetic anisotropy, or stator saturation due to the rotor flux. Based on magnetic saliencies, inject a signal in the non-zero-sequence components, i.e., $\alpha\beta$ or dq. This signal can be a rotating voltage vector, an alternating voltage vector, a pulse pattern or the inherent high-frequency component of the pulse width modulator (PWM). The PWM must be modified to provide excitation when zero voltage is applied. In the other cases, measures must be adopted to avoid a degrading

interaction between the injected signal and the current controller. The response to the injected signal is usually evaluated from the non-zero-sequence current, non-zero sequence current derivative or the zero-sequence voltage [9]. Depending on the injected signal and the measured response, the signal processing to estimate the position can be more or less complex. Methods injecting a rotating or alternating vector, i.e., carrier, require filtering in order to distinguish the carrier response from the controlled current. This introduces an important delay, particularly for low-frequency carriers, which degrades the dynamics of the sensorless control.

This problem is addressed but their proposals require more complex signal processing and are parameter dependent. When the injected signal is a pulse pattern, it must be injected while shortly stopping the PWM. In order to increase the dynamics of the position estimation, the repetition frequency of this pulse pattern must be increased. This, in turn, will increase the perturbation introduced to the controller. To overcome this problem, the inherent excitation of the PWM is used. Here again, a complex signal processing is required. Unlike the Usual methods, where the signal is injected in the $\alpha\beta$ or dq components, in the signal is injected in the zero sequence components, and the response is evaluated from the $\alpha\beta$ currents. This method provides a higher sensitivity, and the signal processing is simple.

HIGH-FREQUENCY MODEL OF THE MOTOR

This chapter discusses the high-frequency model of a PMSM is analyzed. Position of the rotor is varying with low and high frequencies. In the case of motors with surface-mounted magnets the magnet flux produces saturation in the stator. The position estimation has a fast dynamic and no addition audible noise is produced. The response is here evaluated by directly measuring the current derivative, providing a higher signal-to-noise ratio. Evaluate the finally inductance matrix to determine position of the rotor is controlled.

The PMSM can be modeled in the stationary reference frame $\alpha\beta o$ as follows:

$$u = Ri + \frac{d(Li)}{dt} + \omega \begin{bmatrix} -\psi_{PM} \sin(\theta) \\ \psi_{PM} \cos(\theta) \\ -3\psi_{PM} \sin(3\theta) \end{bmatrix} \tag{1}$$

In order to analyze the response to a high-frequency excitation, the current vector will be expressed as

$$i = i_L + i_H \tag{2}$$

Where subscripts L and H denote the low and high –frequency components, respectively. Low implies the fundamental and high the switching frequency. by substituting eqn (2) in (1), it yield $u = Ri_H$

$$+Ri_L + \frac{d(L(i_H + i_L))}{dt} + \omega \begin{bmatrix} -\psi_{PM} \sin(\theta) \\ \psi_{PM} \cos(\theta) \\ -3\psi_{PM} \sin(3\theta) \end{bmatrix} \tag{3}$$

The inductance changes with low frequency and will be assumed constant when compared with the high-frequency component. Moreover, the high-frequency component of the resistive voltage drop will be neglected. Under these assumptions, (2.3) can be simplified.

$$u=L\frac{di_H}{dt}+e_L \tag{4}$$

Being e_L a low-frequency component.

$$e_L=Ri_L+\frac{d(Li_L)}{dt}+\omega\begin{bmatrix}-\psi_{PM}\sin(\theta)\\ \psi_{PM}\cos(\theta)\\ -3\psi_{PM}\sin(3\theta)\end{bmatrix} \tag{5}$$

In the case of motors with surface-mounted magnets, the magnet flux produces saturation in the stator. The consequence is that the inductance matrix L becomes a function of the position.

Considering only the high frequency components i.e, flux sources are assumed constant the magnetic circuit can be solved as:

$$\phi=PF \tag{6}$$

$\phi=[\phi_1,\ldots\phi_6]^T$, $F=[F_1,\ldots F_6]^T$ and

$$P=\begin{bmatrix}p1&0&0&0&0&0\\0&p2&0&0&0&0\\0&0&p3&0&0&0\\0&0&0&p4&0&0\\0&0&0&0&p5&0\\0&0&0&0&0&p6\end{bmatrix} \tag{7}$$

The magneto motive force vector F is related with the current vector i_{ABC} by the winding matrix:

$$F=wi_{ABC} \tag{8}$$

$$w=\frac{N}{2}\begin{bmatrix}1&1&1&-1&-1&-1\\-1&-1&1&1&1&-1\\1&-1&-1&-1&1&1\end{bmatrix}^T \tag{9}$$

The flux vector ϕ is related with the flux linkage λ ABC by:

$$\lambda_{ABC}=L_{ABC}i_{ABC} \tag{10}$$

$$L_{ABC}=w^TPw \tag{11}$$

Substituting eqns (4-6) and (8) into (11) we get inductance matrix as function of the position is obtained.

$$L=\left[\begin{array}{cc|c}L_0-L_1\cos(2\theta)&-L_1\sin(2\theta)&L_1\cos(2\theta)\\-L_1\sin(2\theta)&L_0+L_1\cos(2\theta)&-L_1\sin(2\theta)\\\hline\frac{1}{2}L_1\cos(2\theta)&-\frac{1}{2}L_1\sin(2\theta)&\frac{1}{4}L_0\end{array}\right] \tag{12}$$

Where

$$L_0 = \frac{1}{2}(L_d + L_q) \tag{13}$$

$$L_1 = \frac{1}{2}(L_d - L_q) \tag{14}$$

Being L_d and L_q the direct and quadrature inductance in the rotor-oriented reference frame. By solving for the current derivative, it yields

$$\frac{di_H}{dt} = L^{-1}u - w_L \tag{15}$$

With

$$w_L = L^{-1} e_L \tag{16}$$

In the case that L1<L0, i.e, low saliency, the inverse inductance matrix can be approximated by eqn (12). The left upper sub matrix of (12) is commonly used to estimate the position. However it can be observed that the position-dependent terms in the right upper sub matrix of eqn (12) have higher magnitude. That means, that for a given excitation voltage, a higher signal-to-noise ratio can be obtained by evaluating the response to the zero-sequence component than the response to the α or β components. For higher saliencies for instance L1/L0 >0.1, the approximated inverse inductance matrix eqn (12).

For the exact inverse inductance matrix L^{-1}=A, the elements of the right upper sub matrix are

$$L^{-1} = \frac{1}{L_0^2}\left[\begin{array}{cc|c} L0+L1\cos(2\theta) & L1\sin(2\theta) & -4L1\sin(2\theta) \\ L1\sin(2\theta) & L0-L1\cos(2\theta) & 4L1\sin(2\theta) \\ \hline -2L1\cos(2\theta) & 2L1\sin(2\theta) & 4L0 \end{array}\right]^T \tag{17}$$

In addition to the main position dependent terms with two times the angular frequency of the rotor, now there are terms with four times the angular frequency.

VOLTAGE SOURCE INVERTER

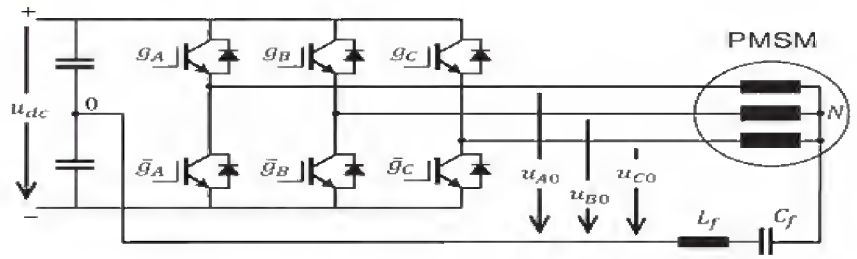

Figure 1: Circuit for the Injection of the Zero-Sequence Carrier, by Using a Standard Space-Vector PWM Controlled Inverter as Source

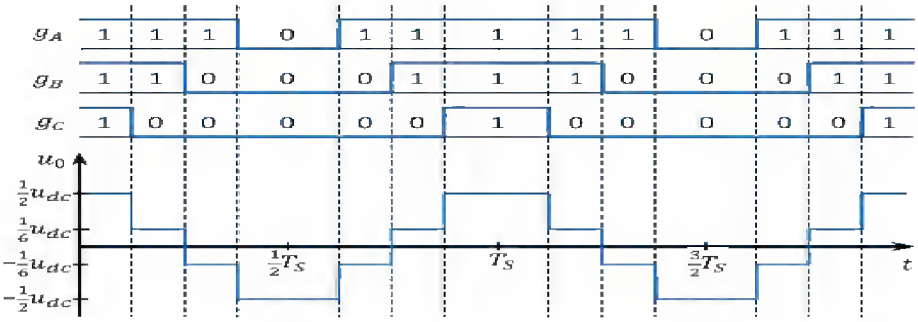

Figure 2: Gate Signals in Standard Space-Vector PWM, and Zero-Sequence Voltage. The Switching Period is Designated by T_S.

Carrier Injection

The response to the zero-sequence voltage must be distinguished from the response to the $\alpha\beta$ voltage. For that reason, a zero-sequence voltage is applied while the $\alpha\beta$ voltages age zero. This happens inherently in an inverter driven with space vector PWM.

By considering the inverter circuit of Figure 1. The zero sequence voltage is defined by

$$u_0 = \frac{1}{3}(u_{A0} + u_{B0} + u_{C0}) \tag{18}$$

The gate signals generated by a standard space-vector PWM and the resulting zero-sequence voltage are shown in Figure 1. It can be seen that the zero vector is generated alternately by the switching states [111] and [000], resulting in zero-sequence voltages udc/2 and -udc/2, respectively. This voltage alternates with the switching frequency. In order to make the zero-sequence voltage acting on the motor windings, the neutral point N must be connected to the dc link point O. However, the space-vector PWM also produces a zero-sequence voltage with three times the fundamental frequency, which would produce a high-current component because of its low frequency. The neutral point is connected to the dc link through a filter, as shown in Figure 1. The filter offers high impedance for up to three times the highest fundamental frequency, and lower impendence for the switching frequency.

The impedance of the filter at switching frequency must be adjusted to limit the zero-sequence current. On one hand, the current must be low enough to avoid excessive losses and, on the other hand the zero-sequence voltage, i.e., the injected signal, must be high enough to provide a good measurable response. The injected voltage should be higher than the voltage drop of the inverter switches, to avoid introducing a distortion during the zero crossing of the current.

Evaluation of the Carrier Response

To evaluate the carrier response, the current derivative is measured at the sampling points t = (1/2)KTs, with k=0,1,2,….,.These sampling points are in the center of the zero states and are commonly used to measure the currents, the voltage at these sampling points is

$$u_K = [0\ 0\ u_c(-1)^K]^T \tag{19}$$

Where u_C is the amplitude of the zero-sequence voltage after the attenuation of the filter.

$$di_{\alpha k} = -4u_c \frac{L_1}{L_0^2} \cos(2\theta)(-1)^K - w_{L\alpha} \quad (20)$$

$$di_{\beta K} = -4u_c \frac{L_1}{L_0^2} \sin(2\theta)(-1)^K - w_{L\beta} \quad (21)$$

The low-frequency components are simply removed by using a high-pass filter. This filter can be easily implemented with the low-frequency component software.

SENSORLESS DIRECT TORQUE CONTROL

Sensorless DTC control for SPMSM is shown as Figure 3. Discusses indirectly control the speed and direct torque control methods and Compensation for motors with high saliencies is used.

A block diagram of the proposed position estimation method is shown in Figure 3. In the upper part, a scheme of a standard drive is shown. The neutral point *N* of the motor is connected to the dc link through a *LC* filter in order to inject the carrier. The carrier produces current components in zero sequence and in the α- and β-axes. However, the instantaneous values of these components, at the sampling instants $t = kT_S/2$, are zero. Consequently, the current measurement for the controller will not be perturbed by the carrier.

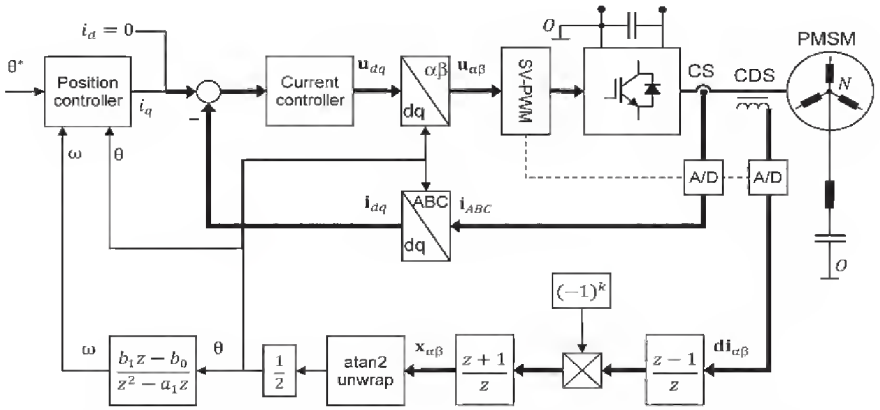

Figure 3: Block Diagram of the Sensorless Position Estimation Method

The information of the rotor angle is comprised in the current derivative at sampling instants $t = kT_S/2$. The current derivative is acquired by a current derivative sensor in Figure 3. Which output is already in the $\alpha\beta$ reference frame ($di_{\alpha\beta}$), as shown in Figure 4.

Instead of using a high-pass filter before the demodulator, a low-pass filter can be used after the demodulator with the same result. In the present proposal, a combination of a simple high-pass filter before and a simple low-pass filter after the demodulator was used, as shown in the lower part of Figure 3. The demodulated and filtered signal $\mathbf{x}_{\alpha\beta}$ is fed to the "atan2" function. The resulting angle, after unwrapping and dividing by two, is the estimated electrical angle. The estimated angle is used for the reference frame transformations and as feedback for the position controller. The speed, which is also used for the position controller, is obtained by differentiating and filtering the estimated position. Alternatively, an observer based on the mechanical model of the machine can be used to estimate the speed.

Current Derivative Sensor

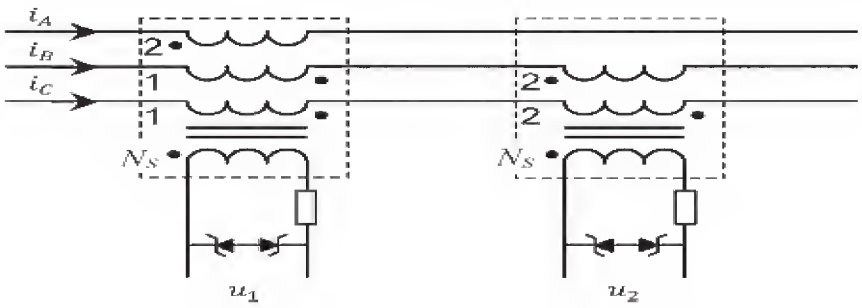

Figure 4: Circuit for Sensing of the Current Derivative in the $\alpha\beta$ Reference Frame

The current derivative sensor consists of a gapped ferrite core with at least two windings. A primary with a small number of turns, from which the current derivative will be measured, and a secondary with a higher number of turns, connected to a high impedance load. The voltage of the secondary is proportional to the current derivative of the primary. The α and β components of the current derivative are directly measured using the circuit of Figure 4.

Compensation for Motors with High Saliencies

If the motors with low saliencies, i.e., $L_1 << L_0$, the demodulated carrier response can be considered as cosine and sine functions, from which the position can be correctly evaluated.

If the motor has high saliency, i.e., $L_1/L_0 > 0.1$, then eqns (12) and (17) must be considered for the inverse inductance matrix. The demodulated carrier response will then result in

$$x_{\alpha k} = -K_1 (L_0 \cos(2\theta) + L_1 \cos(4\theta)) \tag{22}$$

$$x_{\beta k} = K_1 (L_0 \sin(2\theta) + L_1 \sin(4\theta)) \tag{23}$$

With

$$K_1 = \frac{4U_C L_1}{L_0^3 - 3L_0 L_1^2 - 2L_1^3 \cos(6\theta)} \tag{24}$$

It will be assumed that K_1 is constant and approximated by

$$K_1 = \frac{4U_C L_1}{L_0^3 - 3L_0 L_1^2} \tag{25}$$

This is a good approximation for saliencies $L_1/L_0 < 0.35$. Under this assumption, the components of eqns (22) and (23) with four times the angular frequency can be compensated by

$$x'_{\alpha k} = x_{\alpha k} + k_2 (x^2_{\alpha k} - x^2_{\beta k}) \tag{26}$$

$$x'_{\beta k} = x_{\beta k} - K_2 (2 x_{\alpha k} x_{\beta k}) \tag{27}$$

with

$$K_2 = \frac{K_1 L_1}{(K_1 L_0)^2} \tag{28}$$

Substituting and, they yield

$$x'_{\alpha k} = -K_1 \left(\frac{L^3_0 - 2L_0 L^2_1}{L^2_0} \cos(2\theta) + \frac{L^3_1}{L^2_0} \cos(8\theta) \right) \tag{29}$$

$$x'_{\beta k} = K_1 \left(\frac{L^3_0 - 2L_0 L^2_1}{L^2_0} \sin(2\theta) + \frac{L^3_1}{L^2_0} \sin(8\theta) \right) \tag{30}$$

It can be observed that the compensated signals $x'_{\alpha k}$ and $x'_{\beta k}$ contain a main component with two times, and none with four times the angular frequency. A new component with eight times the angular frequency is added by the compensation, but with much smaller amplitude.

The constant K_2 required for the compensation can be obtained by running the estimation methods of Figure 3. The resulting signals $x_{\alpha k}$ and $x_{\beta k}$ contain two frequency components, as can be observed in eqns (22) and (23). The component with lower frequency has amplitude $K_1 L_0$ and its second harmonic has amplitude $K_1 L_1$. These parameters are obtained by a Fourier analysis, and are used in eqn (28). The parameter K_2 needs to be determined only once in the commissioning process. It is also important to determine and compensate any offset present in the signals $x_{\alpha k}$ and $x_{\beta k}$. The position-dependent signals $x_{\alpha k}$ and $x_{\beta k}$ were measured on a motor with high magnetic saliencies.

SIMULATION RESULTS

The simulation modeling of the proposed system and analyze the outputs for the required topologies and the controlled strategies is implemented. Here a controlling technique is simulated with the help of direct torque control and that controlling is going to help in the case generating pulses to the inverter and the complete configuration is simulated for the PMSM.

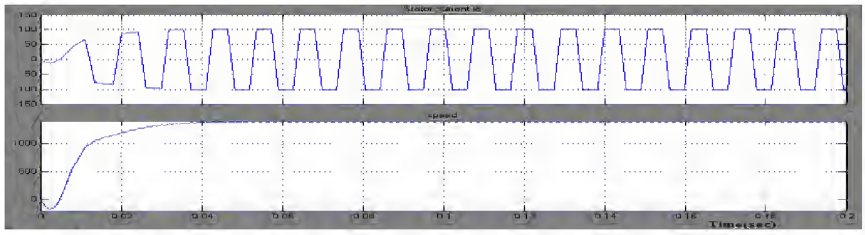

Figure 5: Simulink Output for Stator Current and Speed

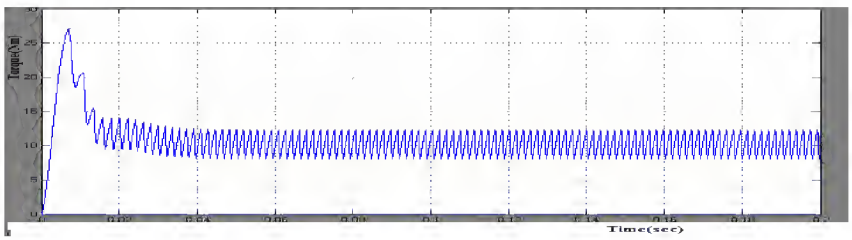

Figure 6: Torque Output

The voltage source inverter shown that DC supply is fed to the inverters by generated SV-PWM. Gate signals directly given to the inverters three phase currents given to PM Synchronous motors then produced higher voltages or lower voltages that is some error or harmonics are produces this are reduces by using the LC filter and with compensation technique .output of the voltage source inverter is Stator currents, stator speed and rotor speed.

Stator current starting having some errors that can be minimized after that constant current is coming for synchronous speed. Speed of the stator and rotor are starting having some harmonics in the surface of the stator it rotates asynchronous speed. The errors are modified based on the zero-sequence carrier injection and using the compensating the output of the LC filter.

Finally sensorless position control of the motor is controlled by the zero-sequence carrier injection and inverter dead time controlled.

Sensorless Direct Torque Control without Compensation

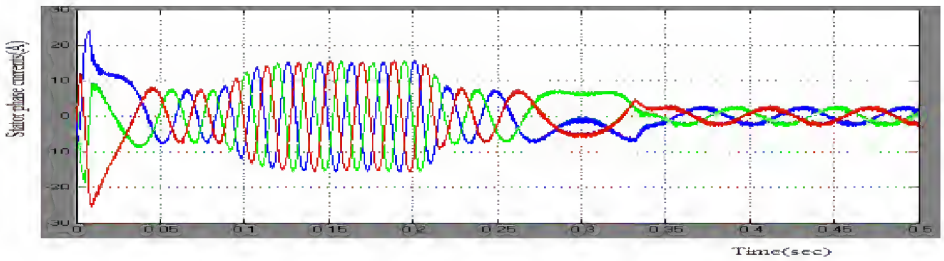

Figure 7: Output for Stator Phase Currents

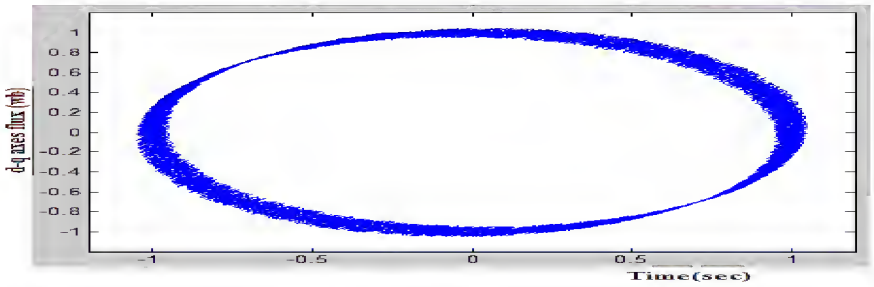

Figure 8: d-q Axes Flux Output

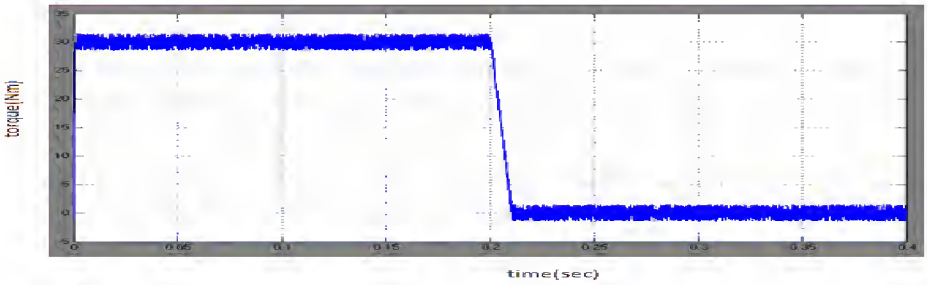

Figure 9: Torque Output

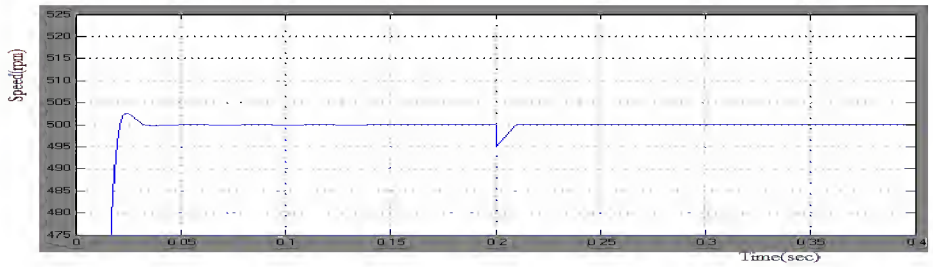

Figure 10: Speed Output

Figure represents the basis block diagram of position estimation of the Motor and direct torque control of PM synchronous motor. In this DTC subsystem consists of references flux and measured flux comparing then produces some error that must be modified then we get commanded signal that will be shown in outputs and torque magnitude error also measured and control of torque ripples that must be shown in outputs. The selection of one switching vector per sampling time depends on magnitude of the flux error and the magnitude of the torque error. Selection of the switching voltage vector is depends on the accurate voltage vector.

These outputs are speed, torque and three phase currents as shown in above outputs. But getting outputs having some error that must be modified by using the compensation technique and LC filter.

Sensorless Direct Torque Control with Compensation

The position is estimated with using the compensation for high saliencies, the estimation error is reduced under constant speed condition. In the transient of speed reversal, the estimation error is still high due to the dynamic load.

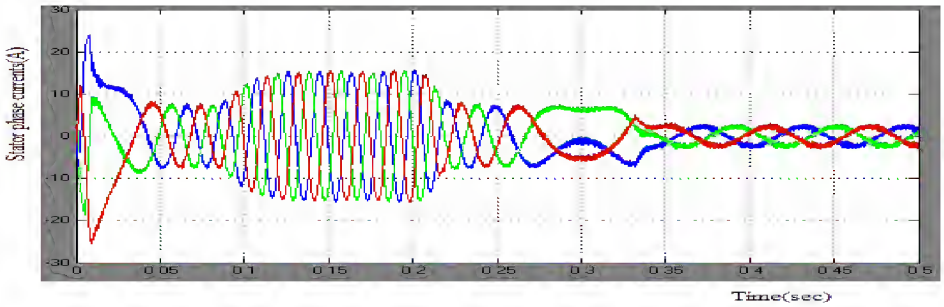

Figure 11: Stator Phase Currents Output

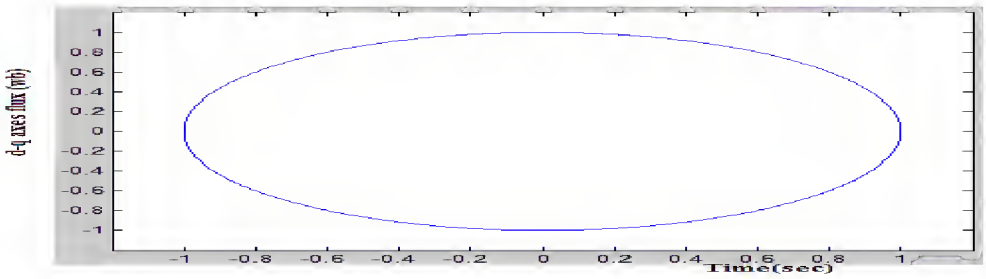

Figure 12: DTC d-q Axes Flux Control Output

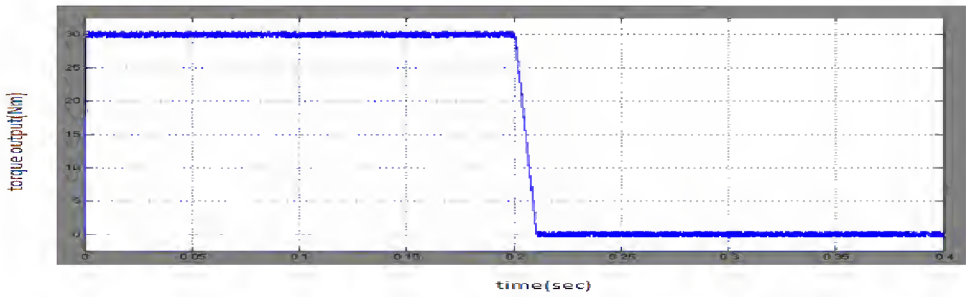

Figure 13: Torque Control Output

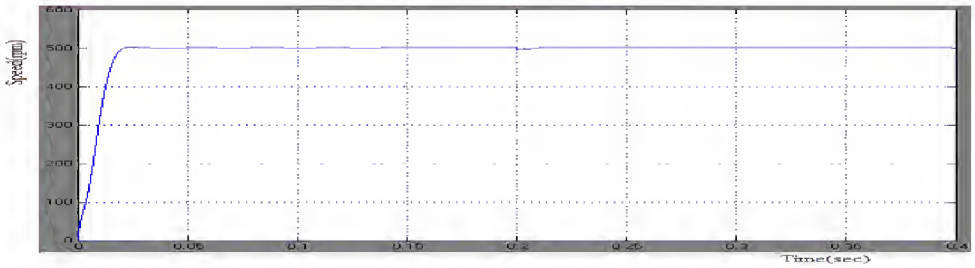

Figure 14: Speed Control Output

Sensorless control of the motor is estimated with using the compensation for high saliencies, the flux errors and torque errors are reduces and Torque control and flux control of PM synchronous motors is obtained.

In a three phase stator currents i_a ,i_b and i_c are contains some disturbances up to 0.35sec after that disturbances are cleared by using LC filter and compensation. In a 0.35sec after that constant three phase currents varying the positive and negative signs.

Torque control output is up to 0.2sec error is having the magnitude constant load torque is taking 30Nm. After that torque ripples are reduces the torque magnitude is also minimized.

Speed of the rotor is controlled the closed loop of the sensorless position is the produces error that can be minimized then constant speed will occurred synchronous speed is rotated.

CONCLUSIONS

Sensorless position control method for PMSMs, using carrier injection in the zero-sequence component and current derivative sensors, has been proposed. The carrier injection does not require any modification of the standard PWM, even when the $\alpha\beta$ voltage is zero. As the carrier is in the zero sequence, it does not interact with the current controller and does not produce torque pulsation. This brings the advantage of not producing any additional audible noise and allowing a high dynamics in the estimation of the position.

The position estimation is not perturbed by the inverter dead time. However, the voltage drop of the inverter switches can produce some perturbation during the zero crossing of the current, in the case that the carrier voltage is too small. In order to implement the sensorless method, some additional hardware is required, comprising an *LC* filter, current derivative sensors, and two additional A/D converter inputs.

Through the comparison between DTC Method without compensation and DTC Method with compensation we have shown that the low dependence on parameters, and makes some improvement in reducing torque ripple, faster

response and stability at wide speed range. Based on the torque ripple criteria, it has been shown from simulation results that the torque ripple is less for the zero-sequence carrier injection method.DTC might be preferred for high dynamic applications, but, shows higher current and torque ripple. Torque ripple is reduced by compensation for high saliencies.

REFERENCES

1. I. Boldea, "Control issues in adjustable speed drives," IEEE Ind. Electron. Mag., vol. 2, no. 3, pp. 32–50, Sep. 2008.
2. J.W. Finch and D. Giaouris, "Controlled ac electrical drives," IEEE Trans. Ind. Electron., vol. 55 no. 2, pp. 481–491, Feb. 2008.
3. R. Leidhold and P. Mutschler,"sensorless position estimation by using the high frequency zero-sequence generated by the inverter," in Proc.35th IEEE IECON.2009.pp, 1282-1287.
4. J.W. Finch and D. Giaouris, "Controlled ac electrical drives," IEEE Trans. Ind. Electron., vol. 55 no. 2, pp. 481–491, Feb. 2008.
5. P. P. Acarnley and J. F. Watson, "Review of position-sensor less operation of brushless permanent-magnet machines," IEEE Trans. Ind. Electron., vol. 53, no. 2, pp. 352–362, Apr. 2006.
6. E. Robeischl and M. Schroedl, "Optimized INFORM measurement sequence for sensor less synchronous motor drives with respect to minimum current distortion," IEEE Trans. Ind. Appl., vol. 40, no. 2, pp. 591–598, 2004.
7. F. M. L. De Belie, P. Sergeant, and J. A. Melkebeek, "A sensor less drive by applying test pulses without affecting the average-current samples," IEEE Trans. Power Electron., vol. 25, no. 4, pp. 875–888, Apr. 2010.
8. T. Kim, H. W. Lee, and M. Ehsani, "Position sensor less brushless DC motor/generator drives: Review and future trends," IET Elect. Power Appl., vol. 1, no. 4, pp. 557–564, Jul. 2007.
9. J.-L. Shi, T.-H. Liu and Y.-C. Chang, "Position control of an interior permanent-magnet synchronous motor without using a shaft position sensor," IEEE Trans. Ind. Electron., vol. 54, no. 4, pp. 1989–2000, Jun. 2007.
10. R. Rauteion of inverter nonlinearity C. Caruana, C. S. Staines, J. Cilia, M. Sumner, and G. M. Asher," Analysis and compensation of inverter nonlinearity effect on a sensorless PMSM drive at very low and zero speed operation,"IEEE Trans.Ind.Electron., vol.57, no.12, pp. 4065-4074, Dec. 2010.